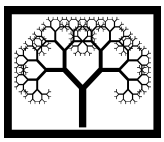
Paper 102



©2003, Civil-Comp Ltd., Stirling, Scotland
Proceedings of the Ninth International Conference
on Civil and Structural Engineering Computing,
B.H.V. Topping (Editor),
Civil-Comp Press, Stirling, Scotland.

Collapse Analysis of Masonry Arch Bridges

T. Aoki† and D. Sabia‡
†Graduate School of Design and Architecture
Nagoya City University, Nagoya, Japan
‡Department of Structural and Geotechnical Engineering
Politecnico di Torino, Turin, Italy

Abstract

The present study deals with the collapse analysis of masonry arch bridges by means of Finite Element Method. Many experimental results on masonry arch bridges show importance of tensile resistance of joints as well as the profile and boundary condition of bridges. In order to analyze and calculate masonry structures, there are several models such as theorem by Castigliano, concrete-like constitutive model, joint element, Bott·Duffin inverse, etc. In this paper, Bott·Duffin inverse is briefly introduced and by means of these models the results obtained from collapse analysis of the masonry arch bridge over Tanaro river, Alessandria in Italy, are discussed.

Keywords: masonry arch bridge, finite element method, collapse analysis, joint element, contact problem, Bott·Duffin inverse.

1 Introduction

Stone and/or brick are usually used as construction materials in Europe from thousands years ago. There are a great number of masonry structures, and eminent examples especially in Italy. Unfortunately, the stability of many of these structures is now threatened by growing fractures and how to repair and maintain for these structures becomes a weighty problem. The repair and maintenance of historical masonry structures require understanding of their structural behaviour particularly up to collapse. A structural model of such masonry material is important for structural analysis by such as Finite Element Method (FEM).

FEM has become one of the most important and useful engineering tools for civil engineers. In order to analyze masonry structures, mathematical models are developed to describe their behaviours. While developing the mathematical models, some assumptions are made for simplification. Definitely masonry material can resist high

compressive stresses but only feeble tensions. Conventional assumptions on masonry are made such that no sliding failure, no tensile strength and infinite compressive strength, and some rigid behaviour due to compression.

The significant steps in the study of arches and domes since the 18th century is discussed with aspect of the logical conclusion of earlier intuitions and pondering [1]. Castigliano has considered that masonry arches consist of two parts, one part must be compressed and the other part needs only be regarded as a load, there is neither compression nor tension. The theory of equilibrium of elastic system is applied to the conditions of imperfectly elastic stresses such as masonry arches for the resisting section [2]. Structural analysis of masonry arches is proposed based on the theorem by Castigliano to find out the form that includes only compressive stresses but no tensile stresses [3]. As an extension of theorem by Castigliano, no-tensile resistant perfect elastic-plastic model is applied on masonry arch bridges [4].

There are mainly two approaches for the analysis of masonry structures by means of FEM, one is macro-modelling and the other is micro-modelling. The most widely used macro-modelling is based on the assumption of isotropy and homogeneity for material, Drucker-Prager plastic failure criterion with low-level cut-off on tensile stresses [5]. Other FEA non-linear models are based on the damage mechanics. Cracks are assumed to form in planes perpendicular to the direction of maximum principal tensile stress which reaches the specified tensile strength. Anisotropic continuum model [6, 7] and continuum model [8] are applied for masonry walls. For sufficiently large structures, the global response of masonry can be well predicted even without the inclusion of the local interaction between the masonry components.

For the micro-modelling of masonry, composite interface model [6], mortar joint model [9], and elastic-plastic joint element [10] are applied for the non-linear behaviour of masonry confining the elastic-plastic failure to mortar bed-joints. As has been shown by the analysis of discontinuous rocks, the joint element is effectively modelled for analyzing structures composed of two different materials with very different strength such as masonry arches. The micro-modelling is capable for describing the local interaction between masonry components, however, it becomes very difficult to solve for sizable masonry structures in which interfaces increase.

Load tests on three spans brickwork arches are conducted with the results in the effect on their behaviour of soil/structure interaction. The influence of spandrel wall stiffening and backfill properties on the failure load and mechanism are also discussed [11, 12]. Full-scale bridges are tested to their collapse with comparison to the finite element plane stress analysis. A thinning method with elimination of tensile areas of the cross section and crushing failure is applied [13].

Based upon the experimental results, an automatic analytical method based on Bott·Duffin inverse to simulate masonry arches as contact problem are presented [14]. The first part of the present study covers a brief introduction of Bott·Duffin inverse [15 - 18]. The second part, by means of theorem by Castigliano, concrete-like constitutive model, joint element, Bott·Duffin inverse, discusses the results obtained from collapse analysis of the masonry arch bridge over Tanaro river, Alessandria in Italy.

2 Bott·Duffin inverse

2.1 Basic equations

Bott·Duffin inverse enables us to present an automatic analytical method for a system of simultaneous linear equations with the subsidiary condition of unknows. In this Chapter, Bott·Duffin inverse is briefly introduced [14 - 18].

Let us consider the minimization problem of the total potential energy function with the subsidiary condition as

$$\prod = \frac{1}{2}\boldsymbol{d}^{\mathrm{T}}\boldsymbol{K}\boldsymbol{d} - \boldsymbol{f}^{\mathrm{T}}\boldsymbol{d} \tag{1}$$

$$\boldsymbol{A}\boldsymbol{d} = \boldsymbol{0} \tag{2}$$

where $\boldsymbol{d}$, incremental displacement vector of order n, $\boldsymbol{K}$, stiffness matrix in the incremental interval of order $n \times n$, $\boldsymbol{f}$, incremental load vector of order n, $\boldsymbol{A}$, subsidiary condition matrix of order $m \times n$, T, symbol of transpose, n, number of degrees of freedom, m, number of subsidiary conditions ($m < n$), respectively.

Lagrange multiplier method can be applied to the analysis of the above minimization problem of Equation (1) with the subsidiary condition of Equation (2). Introducing Lagrange multipliers $\boldsymbol{\lambda}$, this problem becomes the minimization problem of unknowns $n + m$ without the subsidiary condition in which the independent variables are $\boldsymbol{d}$ and $\boldsymbol{\lambda}$. The total potential energy function becomes

$$\prod\nolimits_k = \frac{1}{2}\boldsymbol{d}^{\mathrm{T}}\boldsymbol{K}\boldsymbol{d} - \boldsymbol{f}^{\mathrm{T}}\boldsymbol{d} + \boldsymbol{\lambda}^{\mathrm{T}}\boldsymbol{A}\boldsymbol{d} \tag{3}$$

The stationary conditions of Equation (3) are given by

$$\frac{\partial \prod_k}{\partial \boldsymbol{d}} = \boldsymbol{K}\boldsymbol{d} - \boldsymbol{f} + \boldsymbol{A}^{\mathrm{T}}\boldsymbol{\lambda} = \boldsymbol{0} \tag{4}$$

$$\frac{\partial \prod_k}{\partial \boldsymbol{\lambda}} = \boldsymbol{A}\boldsymbol{d} = \boldsymbol{0} \tag{5}$$

In the above derivation, the relation of $\boldsymbol{K}^{\mathrm{T}} = \boldsymbol{K}$ is used. If we introduce the notation

$$\boldsymbol{r} = \boldsymbol{A}^{\mathrm{T}}\boldsymbol{\lambda} \tag{6}$$

Then Equation (4) takes the form

$$\boldsymbol{K}\boldsymbol{d} + \boldsymbol{r} = \boldsymbol{f} \tag{7}$$

The minimization problem with the subsidiary condition given by Equations (1) and (2) has resulted in the system of equations given by Equations (7) and (5), in other words, simultaneous equations with unknowns $\boldsymbol{d}$ and $\boldsymbol{r}$.

Let us prove the orthogonality condition of $\boldsymbol{d}$ and $\boldsymbol{r}$ by using Equations (5) and (6).

$$\boldsymbol{d}^{\mathrm{T}}\boldsymbol{r} = \boldsymbol{d}^{\mathrm{T}}\boldsymbol{A}^{\mathrm{T}}\boldsymbol{\lambda} = [\boldsymbol{A}\boldsymbol{d}]^{\mathrm{T}}\boldsymbol{\lambda} = \boldsymbol{0} \tag{8}$$

2.2 Bott·Duffin inverse

Let us consider the simultaneous equations given by Equations (7), (5) and (6). The subsidiary condition of Equations (9) and (10) is given by Equation (8).

$$\boldsymbol{d} \in L \tag{9}$$
$$\boldsymbol{r} \in L^{\perp} \tag{10}$$

where L, subspace in linear space R^n of order n, $L^{\perp}$, orthogonal complement to L.

If $\boldsymbol{a}$ is any vector in R^n, P_L and $P_{L^{\perp}}$ are orthogonal projectors on L and $L^{\perp}$, Equations (7) and (8) take the form

$$\boldsymbol{d} = \boldsymbol{P_L a} \tag{11}$$
$$\boldsymbol{r} = \boldsymbol{P_{L^{\perp}} a} = \boldsymbol{f} - \boldsymbol{K P_L a} \tag{12}$$
$$\boldsymbol{P_L} + \boldsymbol{P_{L^{\perp}}} = \boldsymbol{I} \tag{13}$$

where $\boldsymbol{I}$, unit matrix of order $n \times n$. Substituting Equations (11) and (12) into Equation (7), we obtain

$$[\boldsymbol{K P_L} + \boldsymbol{P_{L^{\perp}}}]\boldsymbol{a} = \boldsymbol{f} \tag{14}$$

If the coefficient matrix of order $n \times n$ of Equation (14) is nonsingular, Equations (7) and (8) are consistent for all $\boldsymbol{f}$ and their solutions are unique. In this case, from Equation (14), we get

$$\boldsymbol{a} = [\boldsymbol{K P_L} + \boldsymbol{P_{L^{\perp}}}]^{-1}\boldsymbol{f} \tag{15}$$

Substituting Equation (15) into Equations (11) and (12), and using Equation (7), we obtain

$$\boldsymbol{d} = \boldsymbol{P_L}[\boldsymbol{K P_L} + \boldsymbol{P_{L^{\perp}}}]^{-1}\boldsymbol{f} \tag{16}$$
$$\boldsymbol{r} = \boldsymbol{f} - \boldsymbol{K d} = \boldsymbol{P_{L^{\perp}}}[\boldsymbol{K P_L} + \boldsymbol{P_{L^{\perp}}}]^{-1}\boldsymbol{f} \tag{17}$$

The coefficient matrix of $\boldsymbol{f}$ in the right side of Equation (16) is called "the Bott·Duffin inverse of $\boldsymbol{K}$" and denoted by $\boldsymbol{K}^{(-1)}_{(L)}$, which is orthogonal projector on $\boldsymbol{P_L}$.

$$\boldsymbol{K}^{(-1)}_{(L)} = \boldsymbol{P_L}[\boldsymbol{K P_L} + \boldsymbol{P_{L^{\perp}}}]^{-1} \tag{18}$$

The solution of Equation (7) becomes

$$\boldsymbol{d} = \boldsymbol{K}^{(-1)}_{(L)}\boldsymbol{f} \tag{19}$$
$$\boldsymbol{r} = \boldsymbol{K}^{(-1)}_{(L^{\perp})}\boldsymbol{f} \tag{20}$$

where $\boldsymbol{K}^{(-1)}_{(L^{\perp})}$, is orthogonal projector on $\boldsymbol{P_{L^{\perp}}}$, which is called "the Bott· Duffin inverse of $\boldsymbol{K}$" given by

$$\boldsymbol{K}^{(-1)}_{(L^{\perp})} = \boldsymbol{P_{L^{\perp}}}[\boldsymbol{K P_L} + \boldsymbol{P_{L^{\perp}}}]^{-1} \tag{21}$$

Let us consider the physical meaning of the vector $\boldsymbol{r}$ of order n. In the case of $\boldsymbol{r} = \boldsymbol{0}$, displacement $\boldsymbol{d}$ is given by

$$\boldsymbol{d} = \boldsymbol{K}^{-1}\boldsymbol{f} \tag{22}$$

This displacement, however, is not generally satisfied with Equation (5).

On the other hand, in the case of $\boldsymbol{r} \neq \boldsymbol{0}$, the following equation is obtained by Equation (7)

$$\boldsymbol{d} = \boldsymbol{K}^{-1}[\boldsymbol{f} - \boldsymbol{r}] \tag{23}$$

Substituting Equation (23) into Equation (2), we obtain

$$\boldsymbol{A}\boldsymbol{K}^{-1}[\boldsymbol{f} - \boldsymbol{r}] = \boldsymbol{0} \tag{24}$$

That is, $\boldsymbol{r}$ is virtual external load vector to be satisfied with the subsidiary condition (2). Their solutions of Equations (7), (5) and (6) are obtained uniquely because of the orthogonal condition (8).

3 Masonry arch bridge over Tanaro river, Alessandria in Italy

The bridge of 15 spans brickwork arches over Tanaro river, Alessandria in Italy, is a railway bridge between Turin and Genoa (Figure 1).



Figure 1: Masonry arch bridge over Tanano river, Alessandria in Italy

Each span is about 10 meter and total length of the bridge is about 185 meter. Three arch bridge girders compose the bridge girder. The width of the each arch bridge girder is about 4 meter and the total width of the bridge is about 12 meter. The rise of the

arches is about 1.70 meter and the radical thickness of the brickwork arches is about 0.81 meter (Figure 2). The thickness and width of the pillars are about 2.5 meter and 12 meter, respectively.

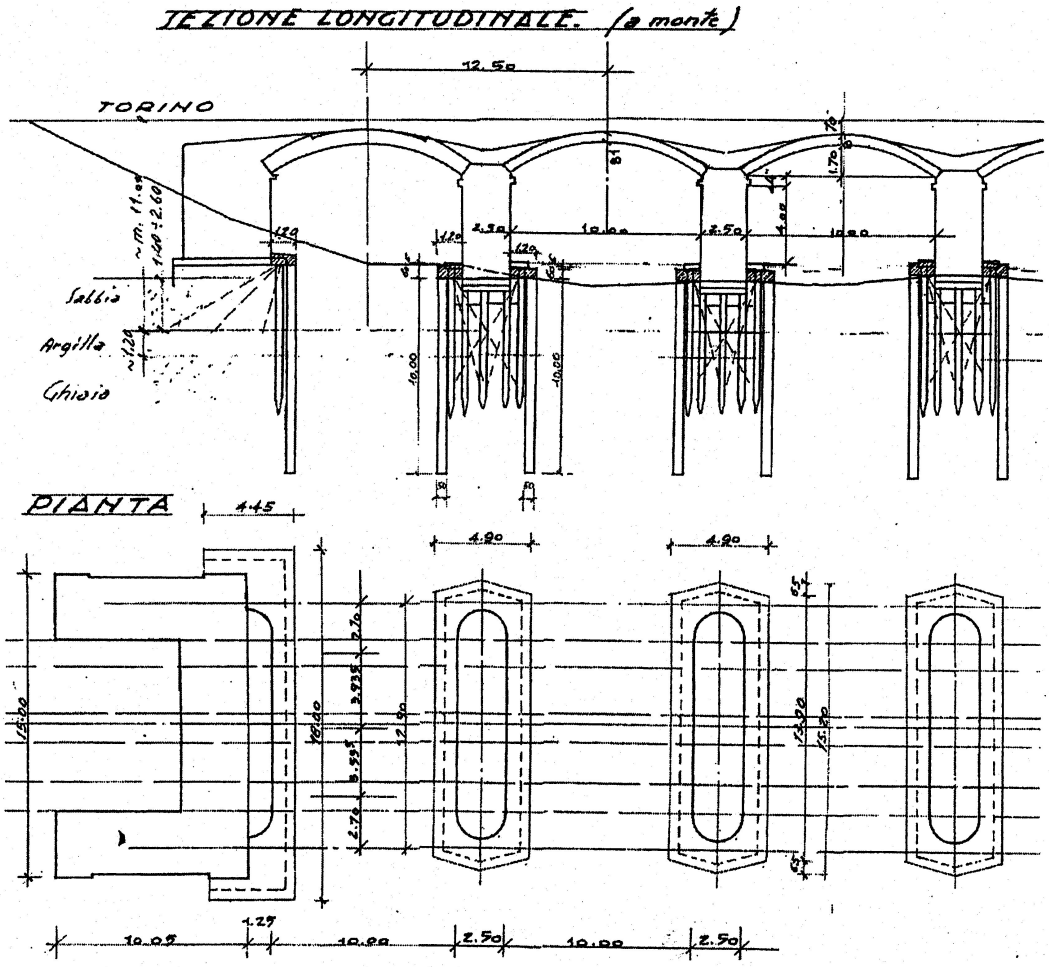


Figure 2: Longitudinal section and plan

4 Numerical examples and discussion

4.1 Analytical models

From the results of the dynamic tests of the masonry arch bridge over Tanaro river, three arch bridge girders behave in different modes even if they are tied by PC bars. Therefore, only one arch bridge girder is discussed here. The Young's modulus, Poisson's ratio and weight per unit volume using in the analysis are $50,000kgf/cm^2$ $(4,903.3N/mm^2)$, 0.15 and $1,800kgf/m^3$ $(0.00001765N/mm^3)$, respectively. The thickness of the arch bridge girder and the pillars are $4m$ and $12m$, respectively. The portion above the masonry arch ring is not taken into consideration.

As shown in Figures 3 to 5, we have prepared three analytical models of the bridge. Model 1 is arch with fixed ends and centric or eccentric load is subjected to the arch (Figure 3). Arch is supported on pillars and the lower parts of the pillars are fixed. Centric load is subjected to the arch (Model 2, Figure 4). Central arch is supported on pillars and outer two arches are supported on both pillar and fixed end. Centric load is subjected to the central arch (Model 3, Figure 5). Length of the load is about 0.8 m in both these three cases.

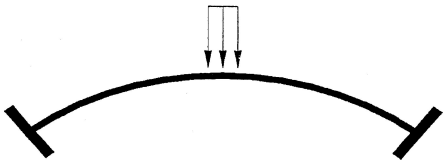


Figure 3: Arch with fixed ends (Model 1)

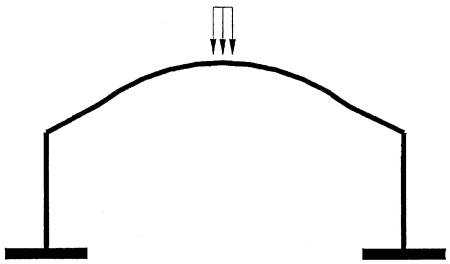


Figure 4: Arch on pillars (Model 2)

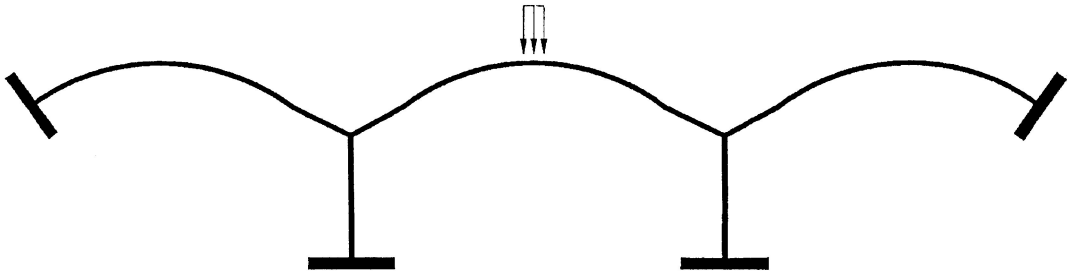
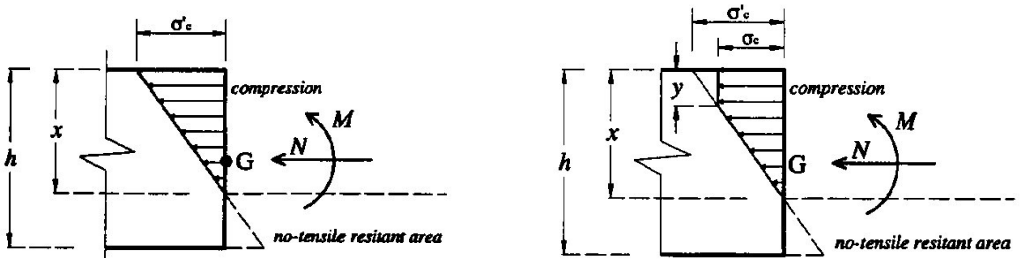


Figure 5: Three arches on pillars (Model 3)



(a) NTR model by Castigliano (1879) (b) NTR perfect elastic-plastic model

Figure 6: No-tensile resistant (NTR) perfect elastic-plastic model by Brencich

4.1.1 No-tensile resistant perfect elastic-plastic model

No-tensile resistant (NTR) model for the voussoirs' interface by Castigliano is shown in Figure 6 (a). The constitutive equations for this model can be derived in terms of the effective section height x. On the other hand, as an extension of theorem by Castigliano, Brencihi et al. proposed no-tensile resistant perfect elastic-plastic (NTR-PEP) model [4] as is shown in Figure 6 (b). Beyond the maximum compressive

strength $f_c{}'$, masonry material will crash in compression when strain $\varepsilon = 2\varepsilon_c$, where ε_c is the strain at the point $\sigma = f_c{}'$. Compressive strength of masonry material used in the analysis is $100kgf/cm^2$ $(9.807N/mm^2)$.

4.1.2 Concrete-like constitutive model

The FEM based on isoparametric degenerated shell elements is adopted for the numerical analysis [19, 20]. The shell element consists of eight layers, the yielding condition of which is given in Figure 7. Figure 8 shows the stress-strain relationship of concrete characterizing the element. Strain hardening of the material after the ultimate strength is ignored, though a small amount of tension stiffening is assumed for the sake of the expediency to achieve numerical efficiency. Cracks are assumed to form in planes perpendicular to the direction of maximum principal tensile stress which reaches the specified tensile strength. The cracked masonry is anisotropic and smeared crack model is adopted.

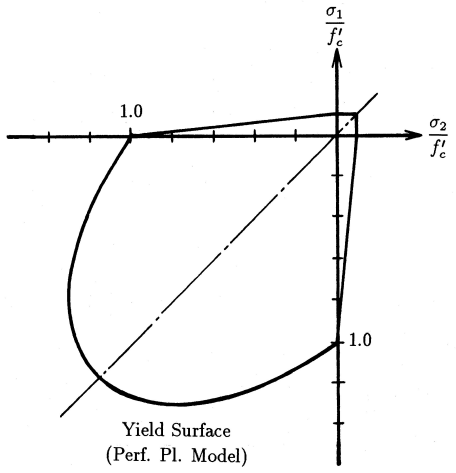


Figure 7: Yielding condition for concrete constitutive model

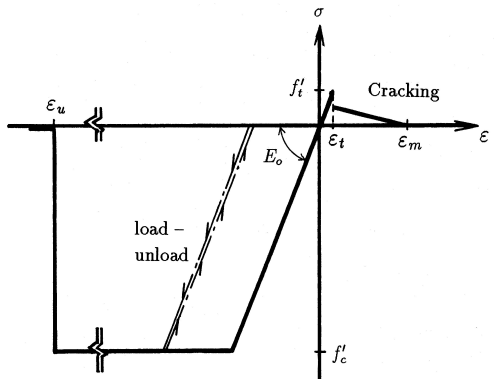


Figure 8: Stress-strain relationship for concrete constitutive model

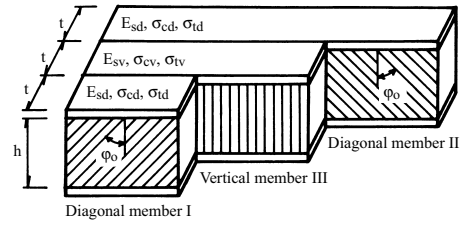


Figure 9: Elastic-plastic joint element composed of three truss-like members

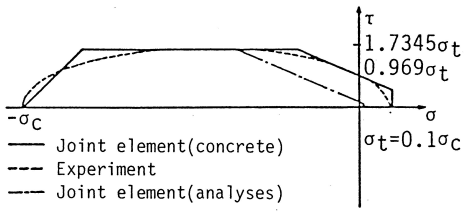


Figure 10: Yielding conditions

4.1.3 Elastic-plastic joint element

As mortar is of relatively low strength compared with brick, the Finite Element analysis (FEA) using the elastic-plastic joint element is much effective. We considered

mortar to be elastic-plastic joint element and brick to be elastic element. The elastic-plastic joint element of the mortar truss members in a two-dimensional situation is illustrated schematically in Figure 9 as a composite model [10]. By introducing a suitable number of members and assigning different material characteristics to each, a variety of sophisticated composite actions can be obtained. But the joint element, herein, consists of three members forming a truss structure.

Figure 10 shows the yielding conditions. The broken line is determined by the experiment of plain concrete under combined stress. Similarly, the yielding condition of the elastic-plastic joint element is represented by the solid line. In due regard to the tensile strength of mortar, however, a strict one represented by a dot-dash-line is applied in FEA. The thickness of the mortar joint used in the analysis is assumed to be 1 mm.

4.1.4 Bott·Duffin inverse

In masonry structures, due to the material properties, only compressive stress is assumed to exist and to a certain extent they become contact problem. Therefore, the thickness of the mortar joint is not taken into consideration.

By means of the Bott·Duffin inverse presented in the previous chapter, the numerical analysis for masonry arch bridge begins with the subsidiary condition $\boldsymbol{Ad} = \boldsymbol{0}$, that is contact state. The tensile force cannot be transmitted between voussoirs, however, the condition $\boldsymbol{r} < \boldsymbol{0}$ needs in masonry structures. The contact state changes into the free state if $\boldsymbol{r} < \boldsymbol{0}$ becomes $\boldsymbol{r} = \boldsymbol{0}$, and then the corresponding nodes will move freely. On the other hand, the shift from the free state to the contact state occurs if the corresponding nodal displacements become the same, and then compressive force can transmit between them ($\boldsymbol{r} < \boldsymbol{0}$). The main advantage of the present method is that it allows the procedure without rebuilding the stiffness matrix $\boldsymbol{K}$ even if the contact state changes. A small amount of the tensile strength due to friction is assumed in FEA.

4.2 Results and discussion

In this chapter, by means of NTR perfect elastic-plastic model, concrete-like constitutive model, elastic-plastic joint element, and Bott·Duffin inverse, the results obtained from collapse analysis of the masonry arch bridge over Tanaro river, Alessandria in Italy are discussed.

Table 1 shows the collapse loads of the masonry arch bridges obtained from the above models. Collapse loads of Model 1, the arch subjected to centric load with fixed ends, are larger than those of Models 2 and 3. Collapse loads of Model 3 are approximately two to three times as much as those of Model 2. In so far as the boundary condition is concerned, Model 3 may be slightly over-idealized, while Model 2 is on the safe side from a structural point of view. From comparison of centric load with eccentric one in Model 1, the latter is more severe than the former in this profile.

Model	NTR-PEP model	Concrete model	EP Joint element	Bott·Duffin inverse
1 Arch with fixed ends (centric load)	650 tf (6374 kN)	808 tf (7924 kN)	735 tf (7208 kN)	698 tf (6845 kN)
1 Arch with fixed ends (eccentric load)	–	283 tf (2775 kN)	131 tf (1285 kN)	198 tf (1942 kN)
2 Arch on pillars (centric load)	70 tf (687 kN)	199 tf (1952 kN)	71 tf (696 kN)	89 tf (873 kN)
3 3 arches on pillars (centric load)	244 tf (2393 kN)	348 tf (3413 kN)	192 tf (1883 kN)	207 tf (2030 kN)

Table 1: Collapse loads of the masonry arch bridges obtained from several models

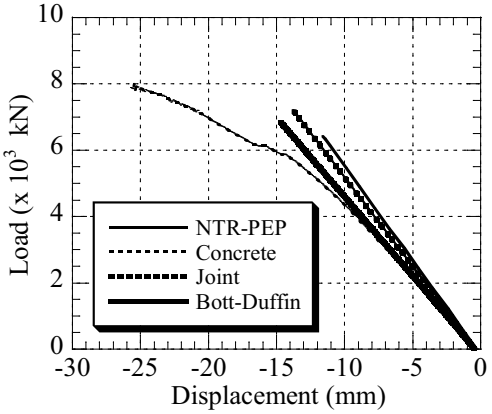


Figure 11: Relationships between load and vertical displacements (Model 1: centric load)

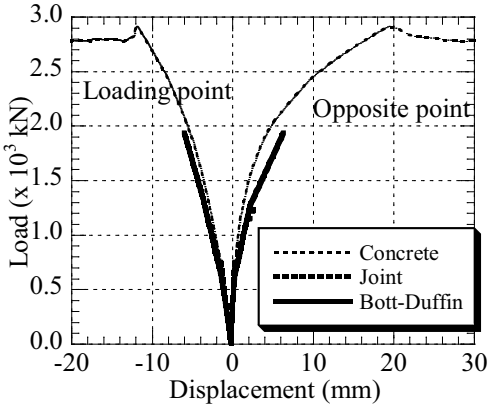


Figure 12: Relationships between load and vertical displacements (Model 2: eccentric load)

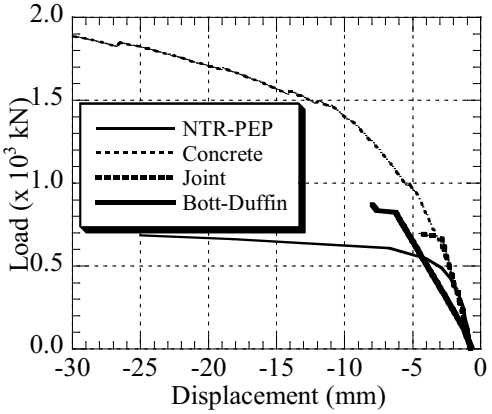


Figure 13: Relationships between load and vertical displacements (Model 2)

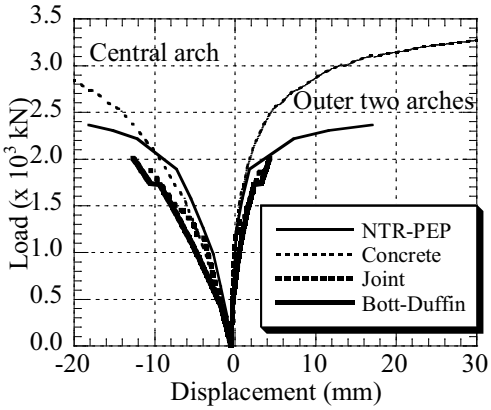


Figure 14: Relationships between load and vertical displacements (Model 3)

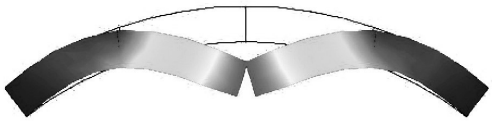


Figure 15: Deformation (Model 1, centric load: Joint element)

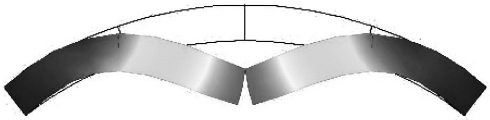


Figure 16: Deformation (Model 1, centric load: Bott·Duffin inverse)



Figure 17: Deformation (Model 1, eccentric load: Joint element)

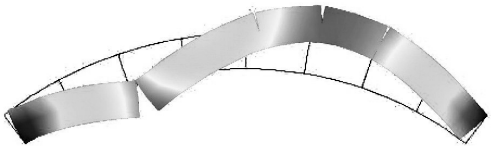


Figure 18: Deformation (Model 1, eccentric load: Bott·Duffin inverse)

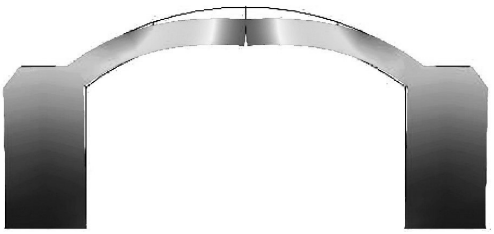


Figure 19: Deformation (Model 2: Joint element)

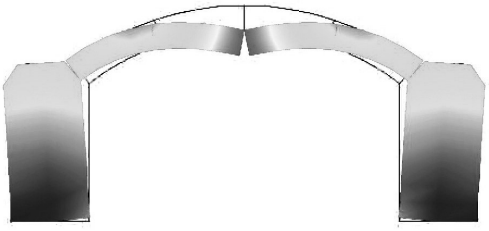


Figure 20: Deformation (Model 2: Bott·Duffin inverse)



Figure 21: Deformation (Model 3: Joint element)



Figure 22: Deformation (Model 3: Bott·Duffin inverse)

The relationships between load and vertical displacements are shown in Figures 11 to 14. Figures 15 to 22 show the deformation of the masonry arch bridge. Solid lines show the original shape. As for the collapse mechanism, there is difference between centric and eccentric loads in Model 1. In the case of centric load, when arch is gradually loaded beyond the tensile strength of masonry material, crack occurs, fracture develops, and at last, the collapse occurs at the center of arch in compression (Figures 15 and 16). The portions at the fixed ends are still sound in this profile. On the other hand, in the case of eccentric load, as shown in Figures 17 and 18, the collapse mechanism due to four hinges occurs in tension. Figures 19 to 22 show the rotation of pillars.

According to the collapse analysis of masonry arch bridges by means of NTR perfect elastic-plastic model, concrete-like constitutive model, elastic-plastic joint element, and Bott·Duffin inverse, there is difference between them. Collapse loads obtained from concrete-like constitutive model are larger than those of the other models. Beyond the tensile strength, masonry material will crack in tension. Smeared crack model is adopted in concrete-like constitutive model, however, the other models are based on discrete crack model. As is shown in Figures 15 to 22, Bott·Duffin inverse is much effective to describe the local interaction between voussoirs. Comparison of those results suggests that the collapse mechanism can well by simulated by the FEA in terms of Bott·Duffin inverse. By introducing a suitable number of the interfaces, more accurate collapse load can be obtained.

5 Concluding remarks

According to the collapse analysis of masonry arch bridges, the FEA using the discrete crack model is more effective than that using the smeared crack model. Bott·Duffin inverse enables us to present an automatic analytical method for a system of simultaneous linear equations with the subsidiary condition of unknowns. The main advantage of the present method is that it allows the procedure without rebuilding the stiffness matrix $\boldsymbol{K}$ even if the contact state changes. Numerical examples show the validity of the Bott·Duffin inverse presented herein for masonry arch bridges as a contact problem.

References

[1] E. Siviero, A. Cecchi, *"A Comment on 18th-Century Studies Attempting to Explain the Statics of Arches and Domes"*, Proc. of the IASS International Symposium on Spatial Structures: Heritage, Present and Future, Vol.2, pp.1289-1298, 1995.

[2] C.A.P. Castigliano, *"Théorie de l'Equilibre des Systèmes Élastiques et ses Applications"*, Turin, Augusto Federico Negro, 1879. Translated by E.S. Andrews, *Elastic Stresses in structures*, London, Scott, Greenwood and Son, 1919. Re-

published with an introduction by G. AE. Oravas, *The Theory of Equilibrium of Elastic Systems and its Application*, New York, Diver, 1966.

[3] T. Aoki, A. Miyamura, S. Di Pasquale, *"Failure Analysis of Masonry Arches"*, Proc. of the 4th International Conference on Computational Structures Technology, Advances in Civil and Structural Engineering Computing for Practice, Civil-Comp Press, Edinburgh, pp.213-219, 1998.

[4] A. Brencich, U.De Francesco, L. Gambarotta, *"Elastic No Tensile Resistant – Plastic Analysis of Masonry Arch Bridges as an Extension of Castigliano's Method"*, Proc. of the 9th Canadian Masonry Symposium, pages 14, 2000.

[5] A. Anthoine, *"Numerical Simulations of Tests Performed on a Masonry Building Prototype"*, Experimental and Numerical Investigation on a Brick Masonry Building Prototype – Numerical Prediction of the Experiment, Report 3.0, G.N.D.T., Pavia, Chapter 7, 1995.

[6] P.B. Lourenço, J.G. Rots, J. Blaauwendraad, *"Two approaches for the analysis of masonry structures: Micro and macro-modeling"*, HERON, Vol.40, No.4, pp.313-340, 1995.

[7] T. Aoki, D. Carpentieri, A. De Stefano, C. Genovese, D. Sabia, *"Analisi Sismica di Parete in Muratura: Metodi e Tecniche a Confronto"*, Proc. of X Convegno Nazionale ANIDIS on L'ingegneria Sismica in Italia, Potenza, pages 12, 2001. (in Italian)

[8] L. Gambarotta, S. Lagomarsino, *"Damage Models for the Seismic Response of Brick Masonry Shear Walls. Part II : The Continuum Model and its Applications"*, Earthquake Engineering and Structural Dynamics, Vol.26, pp.441-462, 1997.

[9] L. Gambarotta, S. Lagomarsino, *"Damage Models for the Seismic Response of Brick Masonry Shear Walls. Part I: The Mortar Joint Model and its Applications"*, Earthquake Engineering and Structural Dynamics, Vol.26, pp.423-439, 1997.

[10] T. Aoki, *"Formulation of Elastic-Plastic Joint Elements and their Application to Practical Structures"*, Computational Modelling of Masonry, Brickwork and Blockwork Structures, ed. by J.W. Bull, Saxe-Coburg Publications, Edinburgh, Scotland, pp.27-52, 2001. This paper is developed from S. Kato, K. Hidaka, T. Aoki, *A Study on the Formulation of a Elastic-Plastic Joint Element by Truss Elements – An Application of the Theory of Effective Strength*, Trans. of A.I.J., No.370, pp.50-59, 1986. (in Japanese)

[11] C. Melbourne, P.J. Walker, *"Load Tests to Collapse of Model Brickwork Masonry Arches"*, Proc. of the 8th Int. Brick and Block Masonry Conference, Vol.2, pp.991-1002, 1988.

[12] C. Melbourne, M. Gilbert, M. Wagstaff, *"The Collapse Behaviour of Multispan Brickwork Arch Bridges"*, The Structural Engineer, Vol.75, No.17, pp.297-305, 1997.

[13] P.C. Das, *"Examination of masonry arch assessment methods"*, Proc. of the IABSE Int. Symposium on Structural Preservation of the Architectural Heritage, pp.385-392, 1993.

[14] T. Aoki, T. Sato, *"Application of Bott·Duffin Inverse to Static and Dynamic Analysis of Masonry Structures"*, Proc. of the 8th Int. Conference on Structural Studies, Repairs and Maintenance of Heritage Architecture 2003, pp.277-286, 2003.

[15] R. Bott, R.J. Duffin, *"On the Algebra of Networks"*, Trans. Am. Math. Soc., Vol.74, pp.99-109, 1953.

[16] M. Domaszewski, A. Borkowski, *"Generalized Inverses in Elastic-Plastic Analysis of Structures"*, J. Struct. Mech., Vol.12, No.2, pp.219-244, 1984.

[17] Y. Hangai, F.L. Guan, *"Structural Analysis of Structures with Constraint Conditions of Displacement by Bott·Duffin Inverse"*, Trans. of A.I.J., No.396, pp.82-96, 1989. (in Japanese)

[18] T. Sato, *"Active Vibration Control Analysis of Building Structures for Earthquake Ground Motions Considering Prescribed Displacement Modes"*, Doctor Thesis of Tohoku University, pages 155, 1999. (in Japanese)

[19] E. Hinton, D.R.J. Owen, *"Finite Element Software for Plates and Shells"*, Pineridge Press, 1984.

[20] T. Aoki, S. Kato, K. Ishikawa, K. Hidaka, M. Yorulmaz, F. Çili, *"Principle of Structural Restoration for Hagia Sophia Dome"*, Proc. of the STREMAH International Symposium, San Sebastian, pp.467-476, 1997.